Acta Tropica 211 (2020) 105595

Contents lists available at ScienceDirect

Acta Tropica

journal homepage: www.elsevier.com/locate/actatropica

Solid lipid nanoparticles as a novel formulation approach for tanespimycin (17-AAG) against *leishmania* infections: Preparation, characterization and macrophage uptake

Vinícius Couto Pires[a], Carla Pires Magalhães[a], Marcos Ferrante[b], Juliana de Souza Rebouças[c], Paul Nguewa[d], Patrícia Severino[e], Aldina Barral[a], Patrícia Sampaio Tavares Veras[a], Fabio Rocha Formiga[f,g,*]

[a] Instituto Gonçalo Moniz, Fundação Oswaldo Cruz (FIOCRUZ), Rua Waldemar Falcão, 121, Candeal, 40296-710, Salvador/BA, Brazil
[b] Departamento de Medicina Veterinária, Universidade Federal de Lavras (UFLA), 37200-000, Lavras/MG, Brazil
[c] Instituto de Ciências Biológicas, Universidade de Pernambuco (UPE), Rua Arnóbio Marques, 310, 50100-130, Recife/PE, Brazil
[d] Instituto de Salud Tropical, University of Navarra, Irunlarrea, 1, E-31008, Pamplona, Spain
[e] Laboratório de Nanotecnologia e Nanomedicina (LNMed), Instituto de Tecnologia e Pesquisa (ITP), Universidade Tiradentes (UNIT), Av. Murilo Dantas, 300, 49010-390, Aracaju/SE, Brazil
[f] Programa de Pós-Graduação em Biologia Celular e Molecular Aplicada, Universidade de Pernambuco (UPE), Rua Arnóbio Marques, 310, 50100-130, Recife/PE, Brazil
[g] Instituto Aggeu Magalhães, Fundação Oswaldo Cruz (FIOCRUZ), Av. Prof. Moraes Rego, s/n, Cidade Universitária, 50670-420, Recife/PE, Brazil

ARTICLE INFO

Keywords:
17-n-allylamino-17-demethoxygeldanamycin (17-aag)
Solid lipid nanoparticles (sln)
In vitro uptake
Macrophages
Leishmaniasis

ABSTRACT

17-N-allylamino-17-demethoxygeldanamycin (17-AAG, tanespimycin) is an inhibitor of heat shock protein 90 (Hsp90), which has been studied in the treatment of cancer such as leukemia or solid tumors. Alternatively, 17-AAG may represent a promising therapeutic agent against leishmaniasis. However, the delivery of 17-AAG is difficult due to its poor aqueous solubility. For exploring the therapeutic value of 17-AAG, we developed solid lipid nanoparticles (SLN) by double emulsion method. SLN exhibited ~100 nm, PDI < 0.2 and zeta potential ~20 mV. In addition, SLN were morphologically spherical with negligible aggregation. The entrapment efficiency of 17-AAG into the lipid matrix reached at nearly 80%. In a separate set of experiments, fluorescent SLN (FITC-labeled) showed a remarkable macrophage uptake, peaking within 2 h of incubation by confocal microscopy. Regarding the drug internalization as critical step for elimination of intracellular *Leishmania*, this finding demonstrates an important feature of the developed SLN. Collectively, these data indicate the feasibility of developing SLN as potential delivery systems for 17-AAG in leishmaniasis chemotherapy.

1. Introduction

The inhibition of heat shock protein 90 (Hsp90) is recognized as an innovative chemotherapeutic approach against cancer (Bhat et al., 2014). In turn, the modulation of Hsp90 has been also reported as a mechanism able to provoke modifications in protozoan parasite differentiation processes. In *Leishmania* spp., inhibition of Hsp90 induces the arrest of promastigote growth and its transformation into rounded amastigote-like forms (Wiesgigl, 2001). Therefore, Hsp90 inhibitors may represent a new generation of anti-leishmanial agents.

Among Hsp90 inhibitors, 17-N-allylamino-17-demethoxygeldanamycin (17-AAG, tanespimycin) **(Fig. 1A)** has been shown to be able to induce the elimination of intracellular *Leishmania* (Petersen et al., 2012). However, the clinical value of 17-AAG has been limited by the poor aqueous solubility, low stability and short biological half-life (Saxena and Hussain, 2013). These hindrances have required a formulation able to improve the therapeutic index of 17-AAG. Nevertheless, parenteral formulations have been prepared with toxic organic excipients such as polyoxyl castor oil (Cremophor® EL), DMSO or ethanol (Xiong et al., 2009).

Different strategies for developing Cremophor-free formulations for 17-AAG have been intended for the treatment of cancer (Saxena and Hussain, 2013; Xiong et al., 2009). On the other hand, a few studies exploring the Hsp90 inhibition by novel 17-AAG formulations against leishmaniasis have been reported (Petersen et al., 2018). With the recognition of 17-AAG as a promising antileishmanial compound, an efficient delivery system able to provide drug internalization into *Leishmania*-infected macrophages is needed, regarding the limitations of 17-

* Corresponding author.
E-mail address: fabio.formiga@fiocruz.br (F.R. Formiga).

https://doi.org/10.1016/j.actatropica.2020.105595
Received 16 March 2020; Received in revised form 21 June 2020; Accepted 21 June 2020
Available online 23 June 2020
0001-706X/

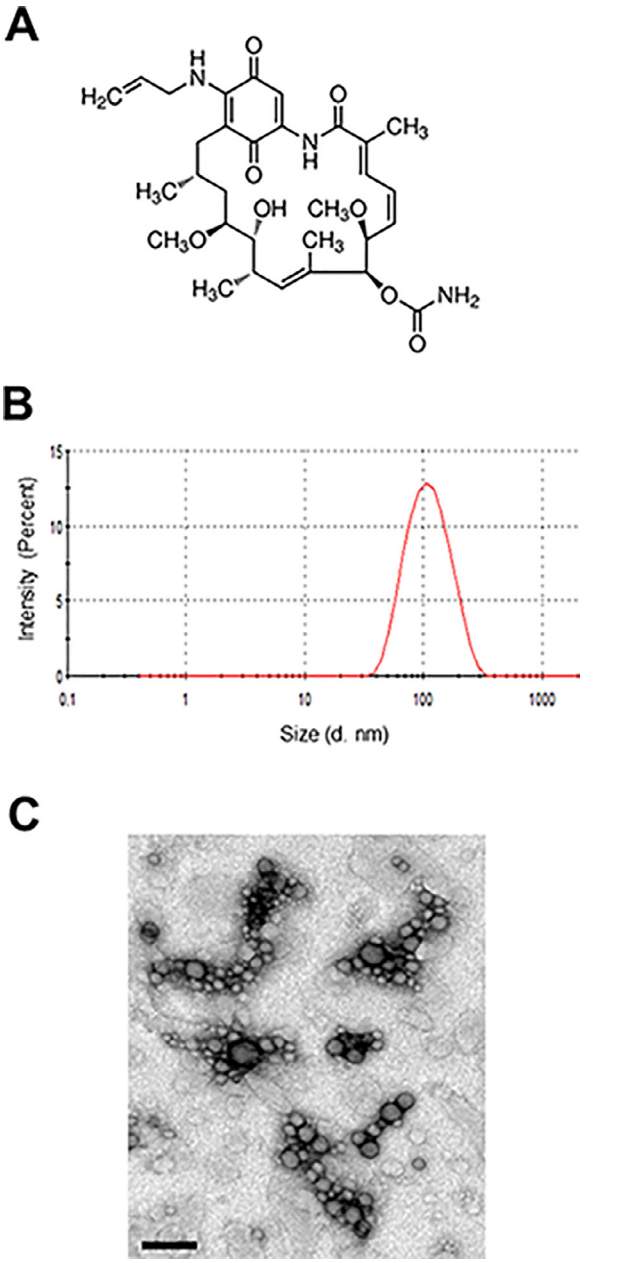

Fig. 1. Chemical structure of 17-AAG (A). Particle size distribution of 17-AAG-loaded SLN by dynamic light scattering (B). TEM microphotograph of SLN loaded with 17-AAG (C). Scale bar: 200 nm.

AAG from formulation standpoint.

Solid lipid nanoparticles (SLN) represent a class of drug delivery systems composed of biocompatible lipids being solid at both room and body temperatures (Paliwal et al., 2020). The first generation of SLN was developed with one solid lipid coated by surfactant. However, due to the low drug loading capacity, the second generation of SLN added a liquid lipid to change the polymorphism characteristic of the matrix. Consequently, an increase on drug solubility and retention into the lipid matrix can be achieved (Andrade et al., 2020).

SLN have attracted major attention as novel colloidal drug carriers for antileishmanial agents. For instance, paromomycin-loaded SLN demonstrated efficacy against L. *major*-infected BALB/c mice (Kharaji et al., 2016). In other approach, lipid-based nanoformulations of trifluralin analogs showed improved performance against L. *infantum* infection in mice (Lopes et al., 2016). Zaioncz and colleagues reviewed the role of colloidal carriers in amphotericin B delivery, highlighting the potential of SLN for the treatment of leishmaniasis (Zaioncz et al., 2017).

In the present study, we have developed and characterized SLN for 17-AAG intravenous delivery. Further, this formulation was tested for its propensity to be internalized by macrophages, which is mandatory for antileishmanial effects. This strategy introduces a novel formulation approach free of toxic excipients, and with potential to provide a safe and effective treatment of leishmaniasis by Hsp90 inhibition.

2. Material and methods

17-AAG was purchased from InvivoGen (San Diego, California, EUA). Glyceryl palmitostearate (Precirol® ATO 5) was kindly gifted by Gattefossé (Saint-Priest, France). β-cyclodextrin, polysorbate 80 (Tween® 80), sorbitan monostearate (Span® 60), fluorescein 5-isothiocyanate (FITC, F7250) and glycerol were provided by Sigma-Aldrich (São Paulo, Brazil). Thioglycollate was purchased from Gibco (Gaithersburg, MD, USA). Dulbecco's modified Eagle's medium (DMEM) was supplied by Lonza (Slough, UK). Ultrapure water (Milli-Q® quality) was used in all the experiments. All other chemicals used were of reagent or pharmaceutical grade.

2.1. Preparation of SLN

17AAG-loaded SLN were obtained by double emulsion method according to composition showed in **Table 1**. Briefly, both the internal water phase (W1) and the lipid phase (LP) were, separately, heated to a temperature 10 °C above the lipid phase transition (melting range for Precirol® ATO 5, 50 – 60 °C). Previously, 17-AAG was solubilized into the LP under magnetic stirring overnight, yielding a clear purple and viscous drug-containing LP. Next, W1 was added to LP under high-shear homogenization using an Ultra-Turrax® T25 homogenizer (IKA, Germany) for 10 min at 10,000 rpm. Then, a primary emulsion was formed, about which a volume of the external water phase (W2) previously cooled (3 °C) was added. This multiple emulsion was homogenized for 2 min at 10,000 rpm. The final volume of W2 was added to multiple emulsion and it was maintained under magnetic stirring for 20 min. For nanoparticle collection, diluted SLN suspensions were placed into Oak Ridge centrifuge tubes and washed two times with ultrapure water by centrifugation at 4 °C (17,000 × *g*, 30 min). Finally, the particles were resuspended in 5 ml of ultrapure water, frozen at –80 °C and lyophilized in a benchtop freeze dryer (FreeZone 2.5, Labconco, USA). All batches were stored at –4 °C. The same procedure was also used to prepare empty SLN (drug-free) and fluorescent SLN containing FITC (10 mg into W1).

2.2. Nanoparticle characterization

SLN were characterized by particle size, zeta potential and transmission electron microscopy (TEM) as described in the Supplementary materials section.

Table 1
Composition of SLN prepared by double emulsion method (w/o/w).

Constituents	Internal water phase (W1)	Lipid phase (LP)	External water phase (W2)
β-cyclodextrin	50 mg		
Precirol® ATO 5		100 mg	
Glycerol		10 ml	
Sorbitan monostearate		50 mg	
17-AAG		10 mg	
Polysorbate 80			250 mg
Distilled water	25 ml		40 ml

2.3. Encapsulation efficiency and drug loading

The 17-AAG encapsulation efficiency (EE) was determined using an indirect method. For that, 17-AAG into SLN was quantified by UV–Vis spectroscopy after separation of free and nanoparticle-associated drug. Samples were obtained by ultra-centrifugation and disruption of SLN with ethanol and vortexing.%EE was calculated by (total drug added – free non-entrapped drug) divided by the total drug added.

2.4. Long-term stability of SLN

Physical stability of SLN suspensions was determined by monitoring pH, electron conductivity and turbidity during 120 storage days at 25 ± 3 °C.

2.5. Uptake assay with fluorescent SLN

Thioglycollate-elicited CBA mouse macrophages were co-incubated with FITC-loaded SLN (1:50 diluted) during 2 h. Thereafter, cells were washed twice with PBS, fixed for 15 min with 2% paraformaldehyde and rinsed in PBS. To visualize nuclei, material was mounted with Vectashield containing DAPI (Vector Laboratories, Burlingame, CA). The slides were examined with a Leica TCS SP8 confocal laser-scanning microscope (Leica Microsystems, Mannheim, Germany).

3. Results and discussion

In this work, we have hypothesized that SLN could provide 17-AAG solubilization without use of toxic excipients. Consequently, this novel formulation could improve the 17-AAG therapeutic index. Herein, SLN were fluid suspensions with white color for empty-SLN or clear purple for 17AAG-loaded SLN. No aggregates or debris were visualized in the nanosuspensions. SLN formulations exhibited sizes around 100 nm with no differences between drug and empty nanoparticles. Narrow particle size distributions were also found, with PDI values < 0.2 **(Fig. 1B).** Of note, incorporation of 17-AAG into SLN did not alter their surface charge, as indicated by similar measurements of zeta potential (ca. –20 mV; **Table 2**). TEM micrographs of SLN revealed the spherical shape of the particles and negligible aggregation **(Fig. 1C).**

The formulation parameters were optimized in order to obtain stable SLN with high 17-AAG loading (not shown). 17-AAG is practically insoluble in water, but soluble in DMSO, methanol and chloroform (~10 mg/ml). To avoid these toxic excipients, glyceryl palmitostearate was selected to produce a lipid matrix able to solubilize properly 17-AAG. Herein, the entrapment efficiency reached at nearly 80% at the drug/lipid ratio of 1:10, resulting in a drug loading around 4%$_{w/w}$. These results of encapsulation efficiency and drug loading were similar those previously reported for 17-AAG loaded-Pluronic® P-123/F-127 mixed micelles, namely about 88% and 4%, respectively (Saxena and Hussain, 2013). But it is worth mentioning these micelles have been designed to deliver 17-AAG in cancer chemotherapy, not for leishmaniasis.

Concerning to SLN stability, **Fig. 2** shows temporal changes in pH, conductivity and turbidity of non-loaded (blank) and 17-AAG-loaded SLN formulations. Consistent reductions on turbidity were determined, with a pronounced effect of 17-AAG on turbidity dropping. These findings correlate with TEM, particle size distribution and surface charge of the SLN formulations, whereas the reduced turbidity of the nanosuspensions could probably indicate a negligible agglomeration of particles in suspension. Therefore, SLN containing 17-AAG were stable for 120 days at 25 ± °C.

As macrophage uptake is a key process for antileishmanial effects, the developed SLN were tested for their propensity for internalization by macrophages. **Fig. 3** shows the macrophage uptake of SLN (green FITC-marked). Intense green fluorescence of SLN could be seen inside the cells. Macrophages recognized SLN as material to be internalized, whereas fluorescent SLN could be seen in projections from the cell surface. In addition, cells displayed a uniform cytoplasmic green fluorescence signal, indicating an effective engulfment of SLN. Hence, the internalization profile of SLN formulations by mouse peritoneal macrophages clearly showed that SLN were highly captured as indicated by the accumulation of the fluorescent marker in cell cytoplasm.

The evaluation of cellular uptake of nanoformulations can be useful to predict their interaction with macrophages in vivo (Lopes et al., 2016). Still, toxicity of anti-*Leishmania* drugs can be reduced by employing macrophage-directed delivery systems. Indeed, targeting antileishmanial agents to macrophages has been reported through various methods, including nanosized drug delivery systems (Van de Ven et al., 2012; Kar et al., 2017). Van de Ven et al. provided in vitro evidence for the passive targeting potential of fluorescently labeled PLGA particles, which were uptake by J774A.1 macrophages infected with L. *donovani* (Van de Ven et al., 2012). Fluorescent coumarin-6-loaded nanostructured lipid carrier also showed considerable internalization in isolated peritoneal macrophage cells, which led to greater antileishmanial activity (Kar et al., 2017). Nanoparticle cellular uptake is markedly dependent on size and surface charge. Nanoparticles in a size range below 200 nm are associated with increased phagocytosis and can be internalized within Leishmania-infected macrophages (Jain et al., 2014). In general, nonphagocytic cells ingest cationic nanoparticles to a higher extent, while phagocytic cells preferentially take up anionic nanoparticles (Fröhlich, 2012). In the present study, macrophages recognized ~100 nm-sized negatively charged SLN as a material to be internalized, probably due to their size, surface charge and lipid nature. Unlike most studies on nanoparticle uptake, we performed an *ex vivo* evaluation of cellular entry of lipid nanoparticles using primary mouse peritoneal macrophages. This is an advantageous uptake evaluation compared to in vitro assays with murine monocyte-macrophage cell lines (e.g. IC-21, J774A.1, RAW 264.7) because it could better reflect the process in vivo.

Seen all together, this investigation led to a SLN-based 17-AAG formulation, which exhibited high 17-AAG loading and stability, and ability for internalization by macrophages. These results indicate the feasibility of SLN as potential delivery systems for 17-AAG, representing an innovative strategy to tackle 17-AAG formulation hurdles.

CRediT authorship contribution statement

Vinícius Couto Pires: Data curation, Investigation, Methodology, Writing - original draft. **Carla Pires Magalhães:** Data curation, Investigation, Methodology. **Marcos Ferrante:** Conceptualization, Data curation, Investigation, Methodology, Writing - original draft. **Juliana de Souza Rebouças:** Data curation, Investigation, Methodology. **Paul Nguewa:** Validation, Visualization, Writing - review & editing. **Patrícia**

Table 2
Nanoparticle characterization data.

Formulation	Particle size (nm)	PDI	Zeta Potential (mV)	Entrapment efficiency (%)	Drug loading* (%)
17AAG-loaded SLN	104.3 ± 1.2	0.18 ± 0.01	– 21.7 ± 0.3	78.3 ± 3.1	4.0 ± 0.8
Blank SLN	116.2 ± 2.4	0.19 ± 0.01	– 18.9 ± 1.2	–	–

* Expressed as mass of incorporated 17-AAG per mass of 17AAG-loaded SLN (%w/w).

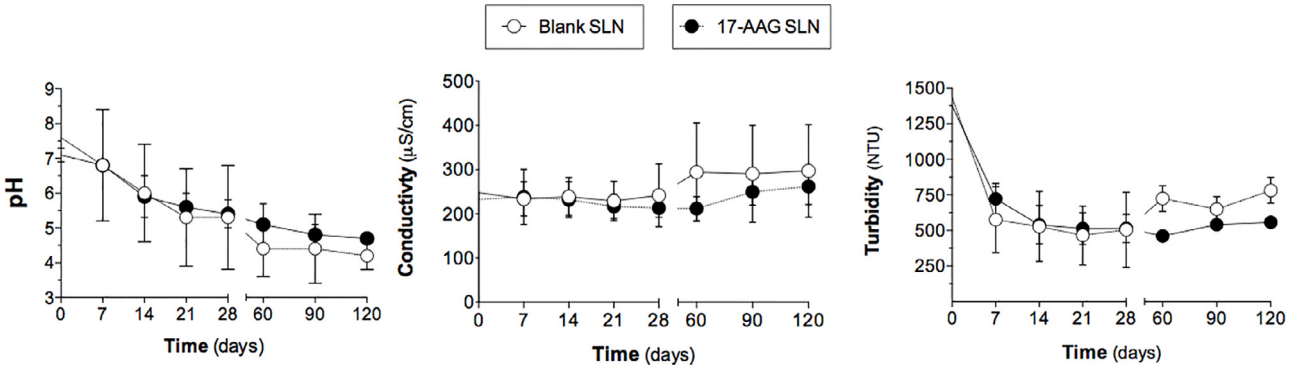

Fig. 2. Stability of SLN during 120 storage days by continuous monitoring of pH, conductivity and turbidity at 25 ± 3 °C.

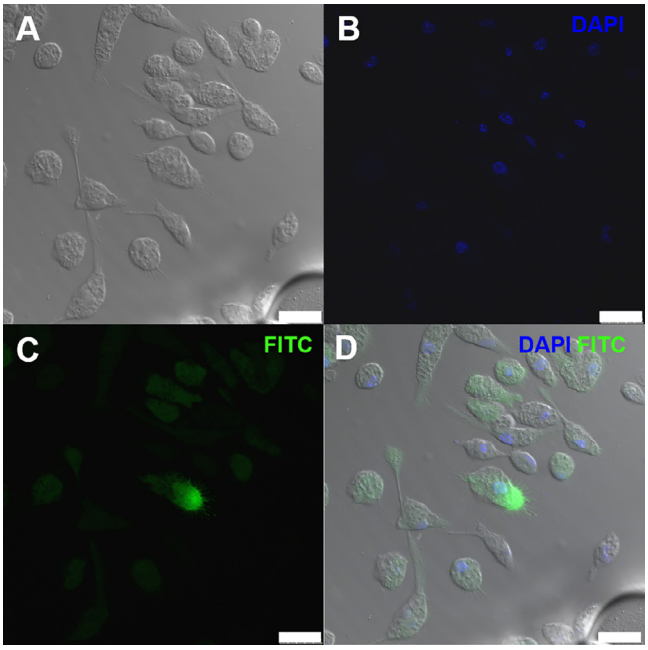

Fig. 3. Confocal images of macrophages exposed to fluorescent SLN in the uptake assay. Contrast microscopy (A) and the corresponding fluorescent field in DAPI and FITC channels (B, C). Merged image showing internalization of SLN into macrophages. Scale bars represent 25 µm.

Severino: Validation, Visualization, Writing - review & editing. **Aldina Barral:** Funding acquisition, Resources, Software, Supervision. **Patrícia Sampaio Tavares Veras:** Conceptualization, Funding acquisition, Resources, Software, Supervision, Validation, Visualization. **Fabio Rocha Formiga:** Conceptualization, Data curation, Investigation, Methodology, Funding acquisition, Resources, Software, Supervision, Validation, Visualization, Writing - original draft, Writing - review & editing.

Declaration of Competing Interest

The authors declare that they have no known competing financial interests or personal relationships that could have appeared to influence the work reported in this paper.

Acknowledgments

This work was supported by the Programa de Excelência Acadêmica – Proex (PgPat/UFBA/FIOCRUZ), INCT-MCTI/CNPq/CAPES/FAPs N° 16/2014 and grants from the Fundação de Amparo à Pesquisa do Estado da Bahia – FAPESB and the Conselho Nacional de Pesquisa e Desenvolvimento Científico – CNPq. PSTV holds a grant from CNPq for productivity in research (307832/2015–5). In addition, this study was financed in part by the Coordenação de Aperfeiçoamento de Pessoal de Nível Superior – Brasil (CAPES) – Finance Code 001. The authors also acknowledge support from the Serviço de Microscopia Eletrônica (SME) – FIOCRUZ/BA for TEM analysis and CIENAM/UFBA for size and zeta potential measurements.

Supplementary materials

Supplementary material associated with this article can be found, in the online version, at doi:10.1016/j.actatropica.2020.105595.

References

Bhat, R., Tummalapalli, S.R., Rotella, D.P., 2014. Progress in the discovery and development of heat shock protein 90 (Hsp90) inhibitors. J. Med. Chem. 57, 8718–8728. https://doi.org/10.1021/jm500823a.

Fröhlich, E., 2012. The role of surface charge in cellular uptake and cytotoxicity of medical nanoparticles. Int. J. Nanomedicine. 7, 5577–5591. https://doi.org/10.2147/IJN.S36111.

Jain, V., Gupta, A., Pawar, V.K., Asthana, S., Jaiswal, A.K., Dube, A., Chourasia, M.K., 2014. Chitosan-assisted immunotherapy for intervention of experimental leishmaniasis via amphotericin B-loaded solid lipid nanoparticles. Appl. Biochem. Biotechnol 174, 1309–1330. https://doi.org/10.1007/s12010-014-1084-y.

Kar, N., Chakraborty, S., De, A.K., Ghosh, S., Bera, T., 2017. Development and evaluation of a cedrol-loaded nanostructured lipid carrier system for in vitro and in vivo susceptibilities of wild and drug resistant Leishmania donovani amastigotes. Eur. J. Pharm. Sci. 104, 196–211. https://doi.org/10.1016/j.ejps.2017.03.046.

Kharaji, M.H., Doroud, D., Taheri, T., Rafati, S., 2016. Drug Targeting to Macrophages With Solid Lipid Nanoparticles Harboring Paromomycin: an In Vitro Evaluation Against L. major and L. tropica. AAPS PharmSciTech 17 (5), 1110–1119. https://doi.org/10.1208/s12249-015-0439-1.

Lopes, R.M., Pereira, J., Esteves, M.A., Gaspar, M.M., Carvalheiro, M., Eleutério, C.V., Gonçalves, L., Jiménez-Ruiz, A., Almeida, A.J., Cruz, M.E., 2016. Lipid-based nanoformulations of trifluralin analogs in the management of Leishmania infantum infections. Nanomedicine (Lond) 11 (2), 153–170. https://doi.org/10.2217/nnm.15.190.

Paliwal, R., Paliwal, S.R., Kenwat, R., Kurmi, B.D., Sahu, M.K., 2020. Solid lipid nanoparticles: a review on recent perspectives and patents. Expert Opin Ther Pat 30 (3), 179–194. https://doi.org/10.1080/13543776.2020.1720649.

Petersen, A.L., Guedes, C.E., Versoza, C.L., Lima, J.G., Freitas, L.A., Borges, V.M., Veras, P.S.T., 2012. 17-AAG kills intracellular Leishmania amazonensis while reducing inflammatory responses in infected macrophages. PLoS One. 7 7, e49496. https://doi.org/10.1371/journal.pone.0049496.

Petersen, A.L.O.A., Campos, T.A., Dantas, D.A.D.S., Rebouças, J.S., da Silva, J.C., de Menezes, J.P.B., Formiga, F.R., de Melo, J.V., Machado, G., Veras, P.S.T., 2018. Encapsulation of the HSP-90 Chaperone Inhibitor 17-AAG in Stable Liposome Allow Increasing the Therapeutic Index as Assessed, in vitro, on Leishmania (L) amazonensis Amastigotes-Hosted in Mouse CBA Macrophages. Front Cell Infect Microbiol 8, 303. https://doi.org/10.3389/fcimb.2018.00303. eCollection 2018.

Saxena, V., Hussain, M.D., 2013. Formulation and in vitro evaluation of 17-allyamino-17-demethoxygeldanamycin (17-AAG) loaded polymeric mixed micelles for glioblastoma multiforme. Colloids Surf B Biointerfaces 112, 350–355. https://doi.org/10.1016/j.colsurfb.2013.07.031.

Van de Ven, H., Vermeersch, M., Vandenbroucke, R.E., Matheeussen, A., Apers, S., Weyenberg, W., De Smedt, S.C., Cos, P., Maes, L., Ludwig, A., 2012. Intracellular drug delivery in Leishmania-infected macrophages: evaluation of saponin-loaded PLGA nanoparticles. J. Drug Target 20, 142–154. https://doi.org/10.3109/1061186X.2011.595491.

Wiesgigl, M.J., 2001. Heat shock protein 90 homeostasis controls stage differentiation in

Leishmania donovani. Mol. Biol. Cell. 12, 3307–3316. https://doi.org/10.1091/mbc.12.11.3307.

Xiong, M.P., Yáñez, J.A., Kwon, G.S., Davies, N.M., Forrest, M.L., 2009. A cremophor-free formulation for tanespimycin (17-AAG) using PEO-b-PDLLA micelles: characterization and pharmacokinetics in rats. J. Pharm. Sci. 98, 1577–1586. https://doi.org/10.1002/jps.21509.

Zaioncz, S., Khalil, N.M., Mainardes, R.M., 2017. Exploring the Role of Nanoparticles in Amphotericin B Delivery. Curr Pharm Des 23 (3), 509–521. https://doi.org/10.2174/1381612822666161027103640.